Electron Delocalization and Charge Transfer in Polypeptide Chains

Ye-Fei Wang,[†] Zhang-Yu Yu,[†,‡] Jian Wu,[§] and Cheng-Bu Liu*[,†]

Institute of Theoretical Chemistry, Shandong University, Jinan 250100 Shandong, China, Heze University, Heze 274015 Shandong, China, and Department of Chemistry, Dalhousie University, Halifax, Nova Scotia, Canada B3H 4J3

Received: March 3, 2009; Revised Manuscript Received: July 10, 2009

In this work, the electron structure and charge-transfer mechanism in polypeptide chains are investigated according to natural bond orbitals (NBO) analysis at the level of B3LYP/6-311++G**. The results indicate that the delocalization of electrons between neighboring peptide subgroups can occur in two opposite directions, and the delocalization effect in the direction from the carboxyl end to the amino end has an obvious advantage. As a result of a strong hyperconjugative interaction, the lowest unoccupied NBO of the peptide subgroup, π^*C−O, has significant delocalization to neighboring subgroups, and the energies of these NBOs decrease from the carboxyl end to the amino end. The formation of intramolecular O···H−N type hydrogen bonds also helps to delocalize the electron from the carboxyl end to the amino end. Thus, the electron will flow to the amino end. The superexchange mechanism is suggested in the electron-transfer process.

1. Introduction

Under the complicated cellular environment, many physical or chemical factors can lead to abnormal changes of DNA structure and alterations of DNA sequence, which are called DNA damages.[1−3] As an important part of cellular biochemistry, DNA repair has to be performed efficiently to maintain the intact genetic information.[4−6] Damage to a single DNA base is commonly repaired by a base excision repair (BER) pathway that removes the damage base and replaces it with a new one.[7−9] Among the BER class of enzymes, MutY, which specifically recognizes 7,8-dihydro-8-oxo-2′-deoxyguanosine/2′-deoxyadenosine (OG/A) mismatches in DNA, is the unique one in that it catalyzes *N*-glycosidic bond hydrolysis to excise a normal base (A) paired with a damaged base (OG).[10−12]

On the basis of the redox activity of the contained $[Fe_4-S_4]^{2+/3+}$ and the long-range charge-transport (CT) theory, Barton et al.[13−16] proposed an important model for the MutY to detect and recognize the DNA damage rapidly. When the binding between MutY and DNA occurs, the oxidation of $[Fe_4-S_4]^{2+}$ drives CT to the DNA duplex. Then, the DNA-mediated CT among oxidized proteins leads to reduction of MutY, which facilitates the dissociation of MutY from DNA and redistribution of MutY along the DNA duplex. Since the DNA-mediated charge transfer cannot proceed through the DNA damage, MutY recognizes the mismatch quickly and efficiently. In this model, $[Fe_4-S_4]^{2+}$ is the electron donor when MutY binds to DNA, and $[Fe_4-S_4]^{3+}$ is the acceptor when MutY dissociates from the DNA duplex. Therefore, the charge transfer along the polypeptide chain, which connects the $[Fe_4-S_4]$ cluster and DNA duplex, becomes a crucial factor in the detecting and recognizing process. Moreover, this process indicates that electron transfer could occur in two opposite directions in the polypeptide chain.

As one of the most important fundamental parts of biochemistry, CT in protein attracts much attention. Gray's group has performed experimental studies on the distance and structural dependence for the charge-transport process in actual protein.[17−19] Their experiments on electron tunneling through organic molecules in frozen glasses provided evidence that covalently bonded pathways can facilitate electron flow through folded polypeptide structures. On the basis of phase space and diffusion theories, Schlag et al.[20] proposed a bifunctional hopping model for charge transport in polypeptides, which was called the waiting and firing mechanism. By employing a molecular dynamical method and density function theory (DFT), the bifunctional model has been used to investigate the CT processes along polypeptides in gas-phase and hydrated media.[21−26] Their studies indicated that the charge transfer through peptides is highly efficient for some choices of amino acid subgroups and that the CT processes are controlled by the internal rotations of Ramachandran angles. Beratan et al.[27−31] developed a per-bond electron tunneling model to identify the dominant electron coupling pathway in protein. Some less important groups are eliminated in this model, and then Hartree−Fock and DFT methods are used to calculate the electron-transfer rates.[32] Their computations revealed the importance of intramolecular hydrogen bonds in the CT process. According to some ab initio DFT[33] and molecular dynamics calculations,[34,35] the long-distance CT in peptides is attributed to a hopping mechanism between neighboring amino acid subgroups. The electronic excitation spectra are well investigated by Head-Gordon et al.[36−38] according to the time-dependent density function theory (TDDFT). In this research, the state crossing the conical intersection presents a highly efficient pathway for long-range charge transfer.

In this work, the polypeptide-mediated charge transfer is investigated by analyzing the electronic structures of the polypeptide chains, and the electron delocalization along polypeptide chains is analyzed by the natural bond orbitals (NBO) technique.[39−44]

* To whom correspondence should be addressed. Tel: 0086 531 88361398. Fax: 0086 531 88564464. E-mail: cbliu@sdu.edu.cn.
† Shandong University.
‡ Heze University.
§ Dalhousie University.

10.1021/jp9020036 CCC: $40.75
Published on Web 09/04/2009

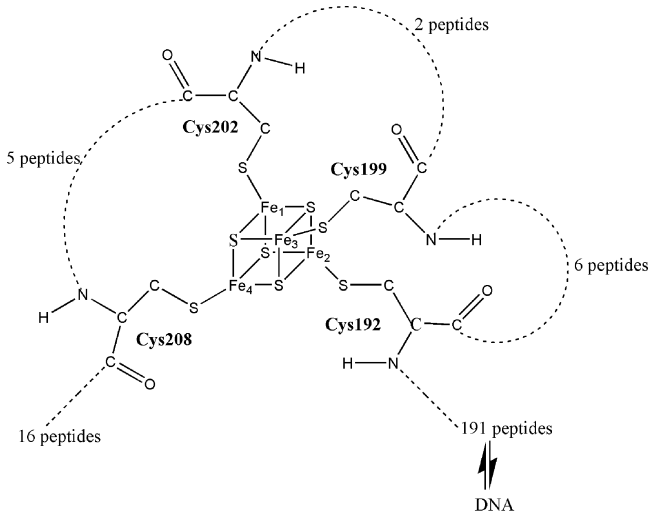

Figure 1. Topology structure of MutY.

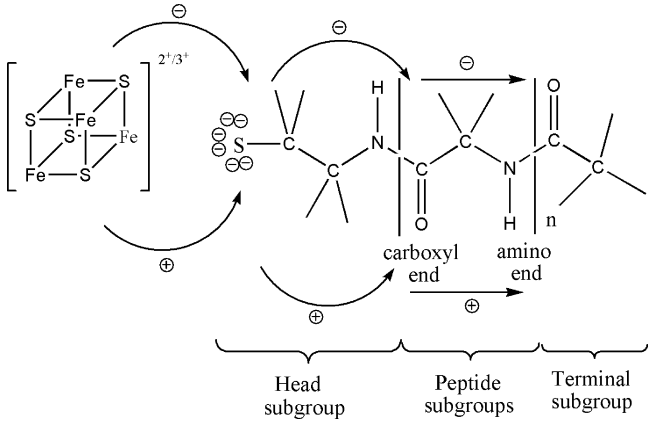

Figure 2. Computational model.

2. Computational Details

The crystal structure of the MutY core fragment at 1.2 Å resolution is taken from the Protein Date Bank (PDB code: 1KG2).[45] As plotted in Figure 1, the peptide chain from Cys192 to Met1 connects the $[Fe_4-S_4]$ cluster and DNA duplex directly. At present, it is impossible to do first-principle density functional calculations for such a large biomolecule. Because of the crucial role of the $[Fe_4-S_4]^{2+/3+}$ cluster described above, a polypeptide chain composed of eight amino acids is truncated from the terminus connecting with the $[Fe_4-S_4]^{2+/3+}$ cluster. All of the side chains connecting with this polypeptide are cut off, and the corresponding dangling bonds are saturated by hydrogen atoms. The final computational model is shown in Figure 2, where n represents the number of amid acid units ($n = 1-7$). To describe it conveniently, the polypeptide chain is divided into three kinds of subgroups, the head subgroup SCH_2CH_2NH- (which connects the carboxyl end of glycine polypeptide), the peptide subgroups Gly_n ($n = 1-7$), and the terminal subgroup $-COCH_3$ (which is used to saturate the amino end of glycine polypeptide). As discussed in the Introduction, the electron transfers in a polypeptide chain are in two opposite directions; direction A is from the carboxyl end to the amino end, and direction B is from the amino end to the carboxyl end.[46]

First, the hydrogen atoms are optimized with B3LYP/6-31G(d),[47−52] and the heavy atoms are fixed to retain the local experimental structures. Second, the NBO analyses are carried out at the level of B3LYP/6-311++G**.[26,32,53−55] All of the calculations are performed with the Gaussian03 package.[56]

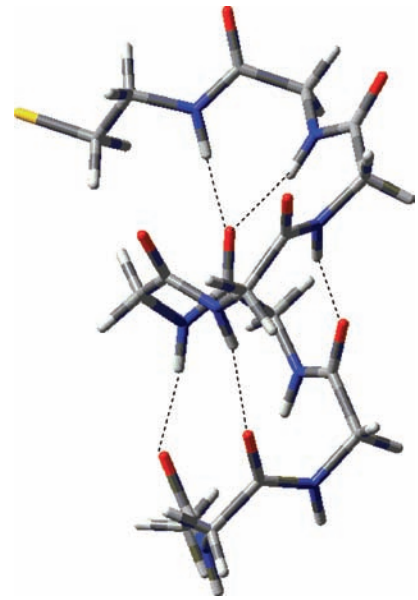

Figure 3. Structure of $[S(CH_2)_2NH-(COCH_2NH)_7-COCH_3]$. The dashed lines represent the intramolecular O···H−N type hydrogen bonds.

3. Results and Discussion

3.1. Electron Delocalization between Subgroups. The natural bond orbital (NBO)[39] is formed from directed orthonormal natural hybrid orbitals (NHOs), which are composed from a set of natural atomic orbitals (NAOs).[40,41] NBOs transformed form ab initio wave functions are found to be in good agreement with Lewis structure concepts. However, the transformation to NBOs also leads to unoccupied non-Lewis-localized orbitals. The most important non-Lewis orbitals are the antibonds which arise from the same set of NAOs that form the bonding NBOs.[42,43] Different from virtual MOs, the antibonding NBOs generally exhibit nonzero occupancies, and their contributions lower the energy.[44] The hyperconjugative interactions between localized Lewis and non-Lewis orbitals lead to a donation of occupancy from bonding and lone pair NBOs to antibonding NBOs.[57] These interactions are the delocalization corrections to the zeroth-order natural Lewis structure and lead to second-order energy lowering, $\Delta E^{(2)}$

$$\Delta E^{(2)}_{\sigma\sigma^*} = -2\frac{\langle\sigma|\hat{F}|\sigma^*\rangle^2}{\varepsilon_{\sigma^*} - \varepsilon_{\sigma}} \qquad (1)$$

where $\langle\sigma|\hat{F}|\sigma^*\rangle$ is the Fock matrix element, approximately proportional to the overlap matrix element. The ε_σ and ε_{σ^*} are the energies of the bonding and antibonding NBOs.[44] It is important to point out that the values of this second-order energy indicate the relative importance of various individual delocalizations; the higher $\Delta E^{(2)}$ value corresponds to stronger delocalization effect.[57] In our following discussion, the $\Delta E^{(2)}$ values are in units of kcal/mol.

As shown in Figure 3, there are five intramolecular O···H−N type hydrogen bonds when the $[S(CH_2)_2NH-(COCH_2NH)_n-COCH_3]$ chain has seven peptides. The distances between O and N atoms range from 2.8 to 3.1 Å; these intramolecular hydrogen bonds belong to the typical moderate hydrogen bonds.[58] Our analyses are based on the individual peptides. Therefore, the delocalization effects between different subgroups will be investigated for two aspects, the delocalizations between

TABLE 1: Total $\Delta E^{(2)}$ Values of All Delocalization Effects between Neighboring Subgroups, as Well as the Dominant Ones[a]

		$n = 1$[e]	$n = 2$[e]	$n = 3$[e]	$n = 4$[e]	$n = 5$[e]	$n = 6$[e]	$n = 7$[e]
head	$N \rightarrow \pi^*C-O$	77.80	75.27	73.84	**84.67**	**83.82**	**83.68**	**83.72**
$\rightarrow$A[b]	$\Delta E^{(2)}_{TA}$[c]	91.46	89.79	88.60	**98.59**	**97.55**	**97.34**	**97.35**
$\leftarrow$B[b]	$O^2 \rightarrow \sigma^*N-C$[d]	18.84	18.82	18.88	18.50	18.58	18.59	18.59
Gly1	$\Delta E^{(2)}_{TB}$[c]	34.14	34.07	34.04	33.75	34.38	34.40	34.37
Gly1	$N \rightarrow \pi^*C-O$		26.33	25.07	**38.61**	**42.94**	**41.36**	**42.07**
$\rightarrow$A[b]	$\Delta E^{(2)}_{TB}$[c]		51.23	50.80	**59.41**	**62.10**	**60.91**	**61.42**
$\leftarrow$B[b]	$O^2 \rightarrow \sigma^*N-C$[d]		20.35	20.29	19.95	19.97	19.99	19.97
Gly2	$\Delta E^{(2)}_{TB}$[c]		40.40	40.13	37.04	36.93	38.04	37.47
Gly2	$N \rightarrow \pi^*C-O$			68.42	68.24	**72.15**	**72.47**	**72.71**
$\rightarrow$A[b]	$\Delta E^{(2)}_{TB}$[c]			81.47	81.81	**85.87**	**86.12**	**86.34**
$\leftarrow$B[b]	$N \rightarrow \pi^*C-O$			20.06	19.91	19.43	19.45	19.45
Gly3	$\Delta E^{(2)}_{TB}$[c]			36.48	36.12	35.57	35.71	35.72
Gly3	$N \rightarrow \pi^*C-O$				61.31	45.29	**69.16**	**68.85**
$\rightarrow$A[b]	$\Delta E^{(2)}_{TB}$[c]				73.44	61.65	**82.09**	**81.72**
$\leftarrow$B[b]	$O^2 \rightarrow \sigma^*N-C$[d]				20.52	20.20	19.74	19.79
Gly4	$\Delta E^{(2)}_{TB}$[c]				36.85	37.09	35.15	35.25
Gly4	$N \rightarrow \pi^*C-O$					71.84	69.77	**77.43**
$\rightarrow$A[b]	$\Delta E^{(2)}_{TB}$[c]					85.24	83.50	**90.81**
$\leftarrow$B[b]	$O^2 \rightarrow \sigma^*N-C$[d]					21.33	21.15	20.72
Gly5	$\Delta E^{(2)}_{TB}$[c]					36.08	35.54	35.08
Gly5	$N \rightarrow \pi^*C-O$						66.29	54.35
$\rightarrow$A[b]	$\Delta E^{(2)}_{TB}$[c]						80.45	71.67
$\leftarrow$B[b]	$O^2 \rightarrow \sigma^*N-C$[d]						18.84	18.57
Gly6	$\Delta E^{(2)}_{TB}$[c]						34.23	34.54
Gly6	$N \rightarrow \pi^*C-O$							64.61
$\rightarrow$A[b]	$\Delta E^{(2)}_{TB}$[c]							78.86
$\leftarrow$B[b]	$O^2 \rightarrow \sigma^*N-C$[d]							18.63
Gly7	$\Delta E^{(2)}_{TB}$[c]							34.17
Gly$n$	$N \rightarrow \pi^*C-O$	60.63	23.16	51.05	65.35	63.40	72.86	66.21
$\rightarrow$A[b]	$\Delta E^{(2)}_{TB}$[c]	75.63	46.65	65.06	79.56	77.38	86.11	78.85
$\leftarrow$B[b]	$O^2 \rightarrow \sigma^*N-C$[d]	20.44	19.92	20.82	21.34	18.67	18.55	20.13
terminal	$\Delta E^{(2)}_{TB}$[c]	36.41	38.43	36.77	35.11	33.52	34.03	34.95

[a] The $\Delta E^{(2)}$ values are in units of kcal/mol. [b] The delocalization effects in polypeptide chains are in two opposite directions; direction A is from the carboxyl end to the amino end, and direction B is from the amino end to the carboxyl end. [c] The total $\Delta E^{(2)}$ values of all delocalization effects between neighboring subgroups in opposite directions are represented as $\Delta E^{(2)}_{TA}$ and $\Delta E^{(2)}_{TB}$. [d] O^2 here means the secondary lone pair of O atoms. [e] The n represents the number of peptide units.

TABLE 2: $\Delta E^{(2)}$ Values of the Delocalization Effects through the Five Intramolecular Hydrogen Bonds[a]

	$O^1{}_5 \rightarrow \sigma^*NH_h$[b]	$O^1{}_5 \rightarrow \sigma^*NH_1$[b]	$O^1{}_6 \rightarrow \sigma^*NH_2$[b]	$O^1{}_7 \rightarrow \sigma^*NH_3$[b]	$O^1{}_t \rightarrow \sigma^*NH_4$[b]
$n = 4$[c]	6.88	3.82			
$n = 5$[c]	7.43	3.45	5.11		
$n = 6$[c]	7.69	3.45	4.73	4.47	
$n = 7$[c]	8.03	3.62	4.65	4.16	3.96

[a] The $\Delta E^{(2)}$ values are expressed in kcal/mol. [b] O^1 expresses the first lone pairs of O atoms, and the subscripts h, 1, 2, 3, 4, 5, 6, 7, and t indicate that the orbital belongs to the head, Gly1, Gly2, Gly3, Gly4, Gly5, Gly6, Gly7, and terminal subgroups, respectively. [c] The n indicates the number of peptide units.

neighboring subgroups along the polypeptide chain and the delocalizations through intramolecular hydrogen bonds.

3.1.1. Delocalizations between Neighboring Subgroups. Similar to the electron-transfer process, this kind of delocalization occurs in two opposite directions. The total $\Delta E^{(2)}$ values[59−61] of all delocalization effects between neighboring subgroups in these two directions are listed in Table 1; their $\Delta E^{(2)}$ values are represented as $\Delta E^{(2)}_{TA}$ and $\Delta E^{(2)}_{TB}$. Meanwhile, a dominant delocalization effect between neighboring subgroups, which has the largest $\Delta E^{(2)}$ value, is also listed. In direction A, the dominant delocalization is that electron moves from the lone pair of N in a anterior subgroup to the lowest unoccupied molecular orbital of the corresponding posterior subgroup, that is, from $(n-1)$N to $(n)\pi^*C-O$. In direction B, the domain delocalization is that the electron moves from the highest occupied molecular orbital of a posterior subgroup to the σ^*N-C orbital of the corresponding anterior subgroup, that is, from $(n)O^2$ to $(n-1)\sigma^*N-C$; here the superscript 2 means the secondary lone pair of O. By comparing the $\Delta E^{(2)}$ values of the above two dominant delocalizations and the $\Delta E^{(2)}_{TA}$ and $\Delta E^{(2)}_{TB}$ values, it is easy to find that the delocalization effects in direction A have an obvious advantage over those in the opposite direction.

3.1.2. Delocalizations through Intramolecular Hydrogen Bonds. The delocalization effects through the five intramolecular hydrogen bonds are reported in Table 2. In this kind of interaction, the electron moves from the first lone pair of O of a posterior subgroup to the σ^*N-H orbital of the corresponding anterior subgroup, that is, from $(n)O^1$ to $(n-1)\sigma^*N-H$. That is to say, the delocalization effect through the intramolecular O···H−N bond is from the amino end to the carboxyl end, or in direction B.

Although the $\Delta E^{(2)}$ values of hydrogen bonds are much lower than those of the hyperconjugative interactions between neighboring subgroups, intramolecular O···H−N bonds play a very important role in the whole delocalization process. As show in Table 1, the $\Delta E^{(2)}$ of the dominant delocalization effect and the total $\Delta E^{(2)}$ in direction A are larger than those in direction B.

TABLE 3: NBO Occupation Numbers of the Orbitals Involved in Dominant Delocalization Effects

	$n = 1^b$	$n = 2^b$	$n = 3^b$	$n = 4^b$	$n = 5^b$	$n = 6^b$	$n = 7^b$
$\pi^*C-O_1{}^a$	0.34	0.34	0.34	**0.36**	**0.35**	**0.35**	**0.35**
$O^2{}_1{}^a$	1.89	1.89	1.89	1.89	1.89	1.89	1.89
$\pi^*C-O_2{}^a$		0.23	0.23	**0.27**	**0.27**	**0.27**	**0.27**
$O^2{}_2{}^a$		1.88	1.88	1.88	1.88	1.88	1.88
$\pi^*C-O_3{}^a$			0.29	0.30	**0.31**	**0.31**	**0.31**
$O^2{}_3{}^a$			1.88	1.88	1.88	1.88	1.88
$\pi^*C-O_4{}^a$				0.28	0.26	**0.31**	**0.31**
$O^2{}_4{}^a$				1.87	1.88	1.88	1.88
$\pi^*C-O_5{}^a$					0.32	0.32	**0.34**
$O^2{}_5{}^a$					1.88	1.88	1.88
$\pi^*C-O_6{}^a$						0.31	0.29
$O^2{}_6{}^a$						1.88	1.88
$\pi^*C-O_7{}^a$							0.30
$O^2{}_7{}^a$							1.88

[a] O^2 means the secondary lone pair of O atoms, and the subscript 1, 2, 3, 4, 5, 6, and 7 indicate that the orbital belongs to Gly1, Gly2, Gly3, Gly4, Gly5, Gly6, and Gly7, respectively. [b] The *n* indicates the number of peptide units.

TABLE 4: Distribution of NBO Charges within Each Subgroup

	head	Gly1	Gly2	Gly3	Gly4	Gly5	Gly6	Gly7	terminal
$n = 1^a$	−0.92729	**−0.05465**							−0.01803
$n = 2^a$	−0.92484	−0.05556	**−0.03592**						0.01635
$n = 3^a$	−0.91696	−0.05256	−0.03847	**−0.03276**					0.04077
$n = 4^a$	−0.90595	−0.05356	−0.04813	−0.03675	**0.03596**				0.00845
$n = 5^a$	−0.81924	−0.04874	−0.02969	−0.04037	0.0141	**−0.06429**			−0.01175
$n = 6^a$	−0.76167	−0.04918	−0.03043	−0.02084	0.01672	−0.05256	**−0.09618**		−0.00589
$n = 7^a$	−0.71678	−0.04911	−0.03182	−0.02235	0.03728	−0.02271	−0.08517	**−0.09643**	−0.01295

[a] The *n* indicates the number of peptide units.

Furthermore, when the polypeptide chains are composed of four peptides, these two kinds of $\Delta E^{(2)}$ values between the head subgroup and the first peptide subgroup and between the first peptide subgroup and the second subgroup increase by 10 kcal/mol suddenly. Increasing the length of the polypeptide chain also increases these $\Delta E^{(2)}$ values between the second and third peptide subgroups, the third and fourth peptide subgroups, and the fourth and fifth peptide subgroups. The increase of $\Delta E^{(2)}$ values is believed to be induced by the increase of the hydrogen bond. In other words, although O···H−N type hydrogen bonds would delocalize the electron from the amino end to the carboxyl end, they also promote the delocalization of the electron from the carboxyl end to the amino end.

3.2. Electronic Structures. ***3.2.1. Occupation Number of Orbitals.*** As mentioned in section 3.1.1, in these two dominant delocalization effects $(n-1)N \rightarrow (n)\pi^*C-O$ and $(n)O^2 \rightarrow (n-1)\sigma^*N-C$, π^*C-O is the lowest unoccupied molecular orbital of each peptide subgroup, and the nO^2 is the highest occupied molecular orbital. The NBO occupation numbers of the antibond π^*C-O and the secondary lone pair oxygen O^2 are listed in Table 3.

As seen from Table 3, the occupation numbers of the antibonds π^*C-O are fairly high, which range from 0.23 to 0.36 e. At the same time, occupation numbers of O^2 decrease about 0.11−0.13 e from the ideal occupation. The results also support that the electron delocalizations in two opposite directions exist, and the high occupation number of π^*C-O indicates the advantage of $(n-1)N \rightarrow (n)\pi^*C-O$ delocalization.

In addition, the occupation numbers of π^*C-O also increase abruptly (marked in bold in Table 3) when the length of the polypeptide chain increases to four. This happens because the intramolecular hydrogen bond forms when the polypeptide chain has four peptides. The result reveals the important roles of the O···H−N type hydrogen bonds again; it is consistent with the conclusion of $\Delta E^{(2)}$ values in Table 1.

3.2.2. Distribution of NBO Charges within Each Subgroup. Intramolecolar hydrogen bonds themselves would delocalize the electron in direction B, that is, from the amino end to the carboxyl end, but they strongly promote the delocalization in the opposite direction, direction A. The direction of electron delocalization from the carboxyl end to the amino end, that is, direction A, is the dominant one. The distribution of NBO charges listed in Table 4 confirms this result.

As shown in Table 4, the negative charge of the head subgroup decreases with the increasing length of the polypeptide chain. Its reduced values ($Head_n - Head_{n-1}$) are 0.00245, 0.00788, and 0.01101 when *n* increases from 2 to 4. The corresponding reduced values are 0.08671, 0.05757, and 0.04489 when the *n* values are 5, 6, and 7, respectively. This phenomenon is attributed to the formation of the intramolecular O···H−N type hydrogen bonds. The charges of the last peptide subgroup also indicate the important effect of the intramolecular hydrogen bonds. As shown in Table 4, the charges of the last peptide subgroup decrease from $n = 1$ to 4, while the values increase abruptly from $n = 5$ to 7.

3.3. Mechanism of Charge Transfer. The mechanism of long-range charge transfer has been investigated extensively.[62−67] Two mechanisms of charge transfer for a rigid system should be concerned here. In the first model, different subgroups are in contact with each other through continuous and delocalized molecular orbitals, and charge transport occurs by superexchange.[66] The second model is discrete hopping. It is presumed that the charge is localized on one subgroup and has no significant electronic overlap with adjacent ones. Thus, the localized charge hops to an adjacent subgroup by a thermally activated process.[67]

As a reasonable approximation, the negative charge transfers through the lowest unoccupied molecular orbital (LUMO) of the peptide subgroups, while the positive charge migrates through the highest occupied molecular orbital (HOMO). The

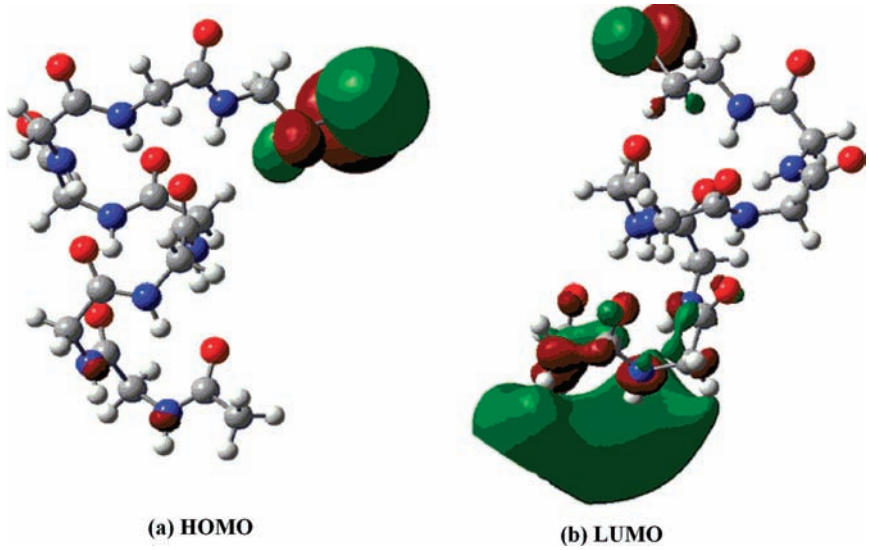

Figure 4. (a) HOMO and the (b) LUMO of $[-S(CH_2)_2NH-(COCH_2NH)_7-COCH_3]$.

TABLE 5: LUMO Energies (au) of Each Peptide Subgroup

	Gly1 π*C−O	Gly2 π*C−O	Gly3 π*C−O	Gly4 π*C−O	Gly5 π*C−O	Gly6 π*C−O	Gly7 π*C−O	terminal π*C−O
$n = 1^a$	0.10668							0.10780
$n = 2^a$	0.10430	0.20824						0.24838
$n = 3^a$	0.10712	0.20350	0.06281					0.08672
$n = 4^a$	0.12270	0.18261	0.07422	0.06758				**0.03536**
$n = 5^a$	0.12452	0.18394	0.08714	0.11446	**0.03352**			**0.04353**
$n = 6^a$	0.12594	0.19340	0.09876	0.08307	**0.04658**	**0.03685**		**0.01289**
$n = 7^a$	0.12775	0.19477	0.10303	0.09205	**0.05350**	**0.06076**	**0.03313**	**0.02431**

[a] The n indicates the number of peptide units.

HOMO and LUMO of $[S(CH_2)_2NH-(COCH_2NH)_7-COCH_3]$ are shown in Figure 4. The LUMO shows a significant delocalization of the π*C−O orbital in Gly7 along the polypeptide chain to neighboring subgroups. However, the orbitals involved in HOMO are unattached localized inner subgroups. Thus, we draw a conclusion that the electron transfer along polypeptide chain adopts the superexchange mechanism, and the thermally activated hopping mechanism will be adopted for the positive charge transfer.

Since the mediated polypeptide chain is extracted from a dissociative protein without DNA, the electron transfer from the Fe−S cluster to the amino end is expected to be easy for an efficient repair process.[68] The energies of the lowest unoccupied NBO in each subgroup are reported in Table 5. As expected, these energies decrease from the carboxyl end to the amino end, except Gly2. Therefore, the negative charge will transfer to the amino end comparatively easily after going through a low-energy barrier, and, the energies of lowest occupied NBO are much lower when the intramolecular O···H−N hydrogen bond is formed (marked in bold). This result is consistent with the change of $\Delta E^{(2)}$ values.

4. Conclusions

As a crucial part of the detecting and recognizing process for MutY, the charge transfer along the polypeptide chain that connects the Fe−S cluster and DNA duplex attracts our attention. In this work, a polypeptide chain is extracted from the crucial area near the Fe−S cluster. The natural bond orbitals (NBO) technique is used to investigate the electron structure and charge-transfer mechanism in this polypeptide chain. The occupation numbers of NBO and the distribution of NBO charges in each individual peptide subgroup are discussed.

The DFT calculations indicate that the electron transfer in the polypeptide chain can occur at two opposite directions, and the electron transfer in the direction from the carboxyl end to the amino end is the dominant one. The lowest unoccupied NBO of a peptide subgroup, π*C−O, has significant delocalization to neighboring subgroups along the polypeptide chain, and their energies decrease from the carboxyl end to the amino end in each unit of the peptide subgroup. Therefore, the electron will flow to the amino end, and the superexchange mechanism is appropriate in the electron-transfer process.

The intramolecular O···H−N type hydrogen bonds play an important role in the electron-transfer process. Although the delocalization direction in the O···H−N bond is from the amino end to the carboxyl end, it is more helpful to promote the delocalization of the electron in the opposite direction.

Acknowledgment. This work is supported by the National Natural Science Foundations of China (Grants 20633060, 20873075) and by the Major State Basic Research Development Programs (Grant 2004CB719902).

References and Notes

(1) Lindahl, T. *Nature* **1993**, *362*, 709.
(2) Berwick, M.; Vineis, P. *J. Natl. Cancer Inst.* **2000**, *92*, 874.
(3) Zhou, B. B. S.; Elledge, S. J. *Nature* **2000**, *408*, 433.
(4) Shigenaga, M. K.; Ames, B. N. *Free Radical Biol. Med.* **1991**, *10*, 211.
(5) Evan, G. I.; Vousden, K. H. *Nature* **2001**, *411*, 342.
(6) Takata, M.; Sasaki1, M. S.; Sonoda, E.; Morrison, C.; Hashimoto, M.; Utsumi, H.; Yamaguchi-Iwai, Y.; Shinohara, A.; Takeda, S. *EMBO J.* **1998**, *17*, 5497.

(7) Krokan, H. E.; Standal, R.; Slupphaug, G. *Biochem. J.* **1997**, *325*, 1.
(8) Scharer, O. D. *Angew. Chem., Int. Ed.* **2003**, *42*, 2946.
(9) David, S. S.; Williams, S. D. *Chem. Rev.* **1998**, *98*, 1221.
(10) Michaels, M. L.; Tchou, J.; Grollman, A. P.; Miller, J. H. *Biochemistry* **1992**, *31*, 10964.
(11) Shibutani, S.; Takeshita, M.; Grollman, A. P. *Nature* **1991**, *349*, 431.
(12) Gogos, A.; Cillo, J.; Clarke, N. D.; Lu, A. L. *Biochemistry* **1996**, *35*, 16665.
(13) Yavin, E.; Boal, A. K.; Stemp, E. D. A.; Boon, E. M.; Livingston, A. L.; O'Shea, V. L.; David, S. S.; Barton, J. K. *Proc. Natl. Acad. Sci. U.S.A.* **2005**, *102*, 3546.
(14) Boal, A. K.; Yavin, E.; Lukianova, O. A.; O'Shea, V. L.; David, S. S.; Barton, J. K. *Biochemistry* **2005**, *44*, 8397.
(15) Gorodetsky, A. A.; Boal, A. K.; Barton, J. K. *J. Am. Chem. Soc.* **2006**, *128*, 12082.
(16) Yavin, E.; Stemp, E. D. A.; O'Shea, V. L.; David, S. S.; Barton, J. K. *Proc. Natl. Acad. Sci. U.S.A.* **2006**, *103*, 3610.
(17) Winkler, J. R.; Gray, H. B. *J. Biol. Inorg. Chem.* **1997**, *2*, 399.
(18) Mayo, S. L.; Ellis, W. R. J.; Crutchley, R. J.; Gray, H. B. *Science* **1986**, *233*, 948.
(19) Gray, H. B. *Science* **2005**, *307*, 99.
(20) Schlag, E. W.; Sheu, S. Y.; Yang, D. Y.; Selzle, H. L.; Lin, S. H. *J. Phys. Chem. B* **2000**, *104*, 7790.
(21) Sheu, S. Y.; Yang, D. Y.; Selzle, H. L.; Schlag, E. W. *J. Phys.Chem. A* **2002**, *106*, 9390.
(22) Lehr, L.; Horneff, T.; Weinkauf, R.; Schlag, E. W. *J. Phys. Chem. A* **2005**, *109*, 8074.
(23) Sheu, S. Y.; Schlag, E. W.; Yang, D. Y.; Selzle, H. L. *J. Phys. Chem. A* **2001**, *105*, 6353.
(24) Kulhanek, P.; Schlag, E. W.; Koca, J. *J. Am. Chem. Soc.* **2003**, *125*, 13678.
(25) Schlag, E. W.; Weinkauf, R. *J. Phys. Chem.* **1996**, *100*, 18567.
(26) Schlag, E. W.; Lin, S. H. *Angew. Chem., Int. Ed.* **2007**, *46*, 3196.
(27) Beratan, D. N.; Onuchic, J. N.; Betts, J. N.; Bowler, B. E.; Gray, H. B. *J. Am. Chem. Soc.* **1990**, *112*, 7915.
(28) Beratan, D. N.; Onuchic, J. N.; Hopfield, J. J. *J. Chem. Phys.* **1987**, *86*, 4488.
(29) Onuchic, J. N.; Beratan, D. N. *J. Chem. Phys.* **1990**, *92*, 722.
(30) Beratan, D. N.; Betts, J. N.; Onuchic, J. N. *Science* **1991**, *252*, 1285.
(31) Onuchic, J. N.; Beratan, D. N.; Hopfield, J. J. *J. Phys. Chem.* **1986**, *90*, 3707.
(32) Prytkova, T. R.; Kurnikov, I. V.; Beratan, D. N. *J. Phys. Chem. B* **2005**, *109*, 1618.
(33) Improta, R.; Antonello, S.; Formaggio, F.; Maran, F.; Rega, N.; Barone, V. *J. Phys. Chem. B* **2005**, *109*, 1023.
(34) Remacle, F.; Ratner, M. A.; Levine, R. D. *Chem. Phys. Lett.* **1998**, *285*, 25.
(35) Jones, G.; Lu, L. N.; Fu, H.; Farahat, C. W.; Oh, C.; Greenfield, S. R.; Gosztola, D. J.; Wasielewski, M. R. *J. Phys. Chem. B* **1999**, *103*, 572.
(36) Dreuw, A.; Head-Gordon, M. *J. Am. Chem. Soc.* **2004**, *126*, 4007.
(37) Dreuw, A.; Worth, G. A.; Cederbaum, L. S.; Head-Gordon, M. *J. Phys. Chem. B* **2004**, *108*, 19049.
(38) Vaswani, H. M.; Hsu, C. P.; Head-Gordon, M.; Fleming, G. R. *J. Phys. Chem. B* **2003**, *107*, 7940.
(39) Foster, J. P.; Weinhold, F. *J. Am. Chem. Soc.* **1980**, *102*, 7211.
(40) Reed, A. E.; Weinhold, F. *J. Chem. Phys.* **1983**, *78*, 4066.
(41) Reed, A. E.; Weinstock, R. B.; Weinhold, F. *J. Chem. Phys.* **1985**, *83*, 735.
(42) Weinhold, F.; Brunck, T. K. *J. Am. Chem. Soc.* **1976**, *98*, 3745.
(43) Brunck, T. K.; Weinhold, F. *J. Am. Chem. Soc.* **1976**, *98*, 4392.
(44) Reed, A. E.; Curtis, L. A.; Weinhold, F. A. *Chem. Rev.* **1988**, *88*, 899.
(45) Gilboa, R.; Kilshtein, A.; Zharkov, D. O.; Kycia, J. H.; Gerchman, S. E.; Grollman, A. P.; Shoham, G. To be published; http://www.rcsb.org/pdb/explore/explore.do?structureId=1KG2.
(46) Galoppini, E.; Fox, M. A. *J. Am. Chem. Soc.* **1996**, *118*, 2299.
(47) Pliego, J. R.; De Almeida, W. B.; Celebi, S.; Zhu, Z. D.; Platz, M. S. *J. Phys. Chem. A* **1999**, *103*, 7481.
(48) Becke, A. D. *Phys. Rev. A* **1988**, *39*, 3098.
(49) Becke, A. D. *J. Chem. Phys.* **1993**, *98*, 5648.
(50) Lee, C.; Yang, W. T.; Parr, R. G. *Phys. Rev. B* **1988**, *37*, 785.
(51) Baboul, A. G.; Curtiss, L. A.; Redfern, P. C.; Raghavachari, K. *J. Chem. Phys.* **1999**, *110*, 7650.
(52) Curtiss, L. A.; Miller, J. R. *J. Phys. Chem. A* **1998**, *102*, 160.
(53) Lii, J. H.; Ma, B. Y. *J. Comput. Chem.* **1999**, *15*, 1593.
(54) Cho, K. H.; Kang, Y. K.; No, K. T.; Scheraga, H. A. *J. Phys. Chem. B* **2001**, *105*, 3624.
(55) Turecek, F.; Chen, X. H.; Hao, C. T. *J. Am. Chem. Soc.* **2008**, *130*, 8818.
(56) Frisch, M. J.; Trucks, G. W.; Schlegel, H. B.; Scuseria, G. E.; Robb, M. A.; Cheeseman, J. R.; Montgomery, J. A., Jr.; Vreven, T.; Kudin, K. N.; Burant, J. C.; Millam, J. M.; Iyengar, S. S.; Tomasi, J.; Barone, V.; Mennucci, B.; Cossi, M.; Scalmani, G.; Rega, N.; Petersson, G. A.; Nakatsuji, H.; Hada, M.; Ehara, M.; Toyota, K.; Fukuda, R.; Hasegawa, J.; Ishida, M.; Nakajima, T.; Honda, Y.; Kitao, O.; Nakai, H.; Klene, M.; Li, X.; Knox, J. E.; Hratchian, H. P.; Cross, J. B.; Bakken, V.; Adamo, C.; Jaramillo, J.; Gomperts, R.; Stratmann, R. E.; Yazyev, O.; Austin, A. J.; Cammi, R.; Pomelli, C.; Ochterski, J. W.; Ayala, P. Y.; Morokuma, K.; Voth, G. A.; Salvador, P.; Dannenberg, J. J.; Zakrzewski, V. G.; Dapprich, S.; Daniels, A. D.; Strain, M. C.; Farkas, O.; Malick, D. K.; Rabuck, A. D.; Raghavachari, K.; Foresman, J. B.; Ortiz, J. V.; Cui, Q.; Baboul, A. G.; Clifford, S.; Cioslowski, J.; Stefanov, B. B.; Liu, G.; Liashenko, A.; Piskorz, P.; Komaromi, I.; Martin, R. L.; Fox, D. J.; Keith, T.; Al-Laham, M. A.; Peng, C. Y.; Nanayakkara, A.; Challacombe, M.; Gill, P. M. W.; Johnson, B.; Chen, W.; Wong, M. W.; Gonzalez, C.; Pople, J. A. *Gaussian 03*; Gaussian, Inc.: Pittsburgh, PA, 2003.
(57) Reed, A. E.; Schleyer, P. R. *J. Am. Chem. Soc.* **1987**, *109*, 1362.
(58) Jeffrey, G. A. *An introduction to hydrogen bonding*; Oxford University Press: New York, 1997.
(59) Hunt, P. A.; Kirchner, B.; Welton, T. *Chem. Eur. J.* **2006**, *12*, 6762.
(60) Yang, Y.; Cui, Q. *J. Phys. Chem. B* **2007**, *111*, 3999.
(61) Sosa, G. L.; Peruchena, N. M.; Contreras, R. H.; Castro, E. A. *J. Mol. Struct.: THEOCHEM* **2002**, *577*, 219.
(62) Newton, M. D. *Chem. Rev.* **1991**, *91*, 767.
(63) Isied, S. S.; Ogawa, M. Y.; Wishart, J. F. *Chem. Rev.* **1992**, *92*, 381.
(64) Schuster, G. B. *Acc. Chem. Res.* **2000**, *33*, 253.
(65) Bixon, M.; Jortner, J. *J. Am. Chem. Soc.* **2001**, *123*, 12556.
(66) Turro, N. J.; Barton, J. K. *J. Biol. Inorg. Chem.* **1998**, *3*, 201.
(67) Ly, D.; Kan, Y.; Armitage, B.; Schuster, G. B. *J. Am. Chem. Soc.* **1996**, *118*, 8747.
(68) Gorodetsky, A. A.; Boal, A. K.; Barton, J. K. *J. Am. Chem. Soc.* **2006**, *128*, 12082.

JP9020036